

Automatic Features Extraction from the Optic Cup and Disc Segmentation for Glaucoma Classification

Marcus Oliveira[1], Cleverson Vieira[1], Ana Paula De Filippo[3], Michel Carlo Rodrigues Leles[1], Diego Dias[1(✉)], Marcelo Guimarães[2], Elisa Tuler[1], and Leonardo Rocha[1]

[1] Universidade Federal de São João del Rei (UFSJ), São João del Rei, Brazil
{mleles,diegodias,etuler,lcrocha}@ufsj.edu.br
[2] Universidade Federal de São Paulo (UNIFESP), São Paulo, Brazil
marcelo.paiva@unifesp.br
[3] Centro de Estudos e Pesquisas Oculistas Associados (CEPOA), Rio de Janeiro, Brazil

Abstract. Glaucoma is a disease that progressively affects the optic nerve, the leading cause of blindness worldwide. One of the most assertive strategies to make the diagnosis is Optical Coherence Tomography (OCT) which identifies anomalies in the anatomy of the optic nerve. OCT is a high-cost exam, so some works in the literature have been using computationally expensive deep neural networks to analyze images on retinal fundus images to diagnose glaucoma. As an alternative to these approaches, in this work, we propose a low-cost computational method for extracting characteristics of the optic nerve anatomy (i.e., optic cup and disc segmentation) through the processing of retinal fundus images, which is used in conjunction with lower computational cost classification algorithms (i.e., support vector machine (SVM)), is capable of performing accurate diagnoses. The most dominant attributes were identified using shapely adaptive explanations (SHAP) and local interpretable model-agnostic explanations (LIME) analysis. More specifically, the more precise the extraction of features, the greater the accuracy of the classifier.

Keywords: Data Mining · Automatic Glaucoma Classification · Feature Extraction

1 Introduction

Glaucoma is a difficult-to-diagnose eye disease and the leading cause of irreversible blindness worldwide. According to [20], glaucoma affects the optic nerve progressively. It is commonly detected by three approaches: detection of increased intraocular pressure, identification of the normal field of vision, and

This work was partially funded by CNPq, CAPES and Fapemig.

© The Author(s), under exclusive license to Springer Nature Switzerland AG 2023
O. Gervasi et al. (Eds.): ICCSA 2023, LNCS 13956, pp. 550–563, 2023.
https://doi.org/10.1007/978-3-031-36805-9_36

assessment of optic nerve damage by calculating the cup-to-disc ratio (CDR). The first approach is the most commonly used in ophthalmic offices because it is easy to perform the evaluation. However, false negative diagnoses are common because the intraocular pressure can remain unchanged at all stages of the disease. The second approach is dependent on complementary exams to evaluate the visual field. On the other hand, the third approach is usually more effective and precise in the diagnosis, performed by fundoscopy, that is, evaluation of detailed images of the optic nerve, identifying possible alterations in its anatomy, more precisely by the vertical increase of the optic disc cup. The optic nerve head evaluation is one of the most clinically effective screening techniques for glaucoma. In this evaluation, some measurements are proposed as clinical conditions for glaucoma screening, such as the vertical cup-to-disc ratio (CDR), disc diameter, rim area, and inferior-superior to nasal-temporal (ISNT) [21] rule. In order to obtain accurate measurements, it is necessary to submit the patient to an examination known as optical coherence tomography (OCT) [23], which in turn has a high cost.

Some machine learning models are being used in various fields of research [3,4,6]. In this way, as an alternative to the OCT exam, we observed some work proposals that use ophthalmologic images of the retinal fundus as a data source for algorithms based on neural networks, which can automatically analyze the anatomical characteristics of the optic nerve and make a possible diagnosis of the eye evaluated [22]. Despite being very assertive, these proposals are limited by some issues, among them: 1) they need a large number of previously classified samples for training; 2) they have a high computational cost, requiring, for example, ophthalmological offices to be equipped with processing servers; and 3) they make predictions with little or no explainability. This last one is the most important since the ophthalmologist needs to understand why the diagnosis was presented to his patient.

This paper proposes an alternative solution to the three existing approaches. Our proposal aims to extract from ophthalmic images the anatomical features of the optic nerve and the segmentation of the optic cup and disc. This information should then be used by computationally less expensive automatic classification algorithms, in which their predictions can be explainable from the extracted and analyzed features. In simplified form, the solution segments the disc and optic cup by processing retinal fundus images and comprises four steps. In the first step, we scan the eye image to locate the optic nerve region (region of interest). In the second step, we process the image by applying the contrast-limited adaptive histogram-limited equalization (CLAHE) algorithm from the scikit-image library [24] for a local contrast enhancement of the images. This algorithm works by dividing the image into rectangular sections and computing the histogram for each section. The intensity values of the pixels are redistributed to improve the contrast and enhance the details of the images. In the third step, we segment the optical disk (delimiting its edges). Our algorithm loads the enhanced/equalized image, binarizes it, removes noise (edge pixels), extracts the points referring to the largest contour of the image using the method findContour, from the

OpenCV library [1], and draws a rectangle marking the extremities of the contour found. This way, the segmentation of the optical disk is performed. In the fourth stage, the cutout region (excavated) segmentation is performed using the same principle of segmentation of the optic disc but with other values of threshold seeking greater emphasis on the internal region, with greater luminosity, also removing noise. The central space in the optic nerve (excavated region), determined by the absence of nerve fibers, is used to extract the anatomical characteristics of the optic nerve, such as CDR, disc diameter, border area and border area and ISNT rule [27].

We evaluated our solution on a dataset with different previously diagnosed images by analyzing the quality of the extracted features in conjunction with the support vector machine (SVM) classification algorithm. The most dominant features were identified using shapely adaptive explanations (SHAP) and local interpretable model-agnostic explanations (LIME) analysis. In our results, we observed that the more accurate the feature extraction is, the higher the accuracy of the classifier will be. On the other hand, the worse the quality of the images, the more difficult our strategy is to extract the features correctly. That points us in the direction of further research to improve some steps of the proposal and its comparison with various databases with images of different quality and thus establish the limits of our solution.

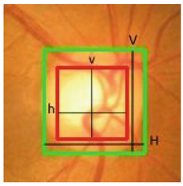
2 Theoretical Framework

Glaucoma can be characterized by a change in the structure of the optic nerve, more specifically in the optic disc, which is the area in which the optic nerve connects to the eye. The optic disc can be divided into two parts: (1) the optic cup, which is in the center of the optic disc as a bright circular area and; (2) the peripheral region around the cup, which is the neuroretinal rim. The optic disc changes visually when the optic nerve fibers are damaged due to glaucoma; this leads to enlargement of the cup region called cupping and is an indicator for detecting suspected glaucoma [20].

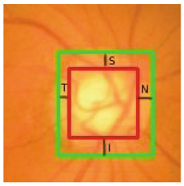
There are some quantitative strategies to evaluate the structure of the optic nerve. One is the vertical CDR, which corresponds to the vertical cup diameter (VCD) ratio to the vertical disc diameter (VDD). Figure 1 depicts the metric – (a), where the VCD is indicated by the letter v and the VDD is indicated by the letter V. The CDR measures the widening of the cup relative to the disc (thinning of the neuroretinal rim). The greater the CDR, the greater the risk for glaucoma [12,27].

Another quantitative strategy used to differentiate the normal optic nerve from the glaucomatous optic nerve is the ISNT rule. In normal eyes, the inferior (I) disc edge thickness is greater than the superior (S) edge thickness which is greater than the nasal (N) edge thickness, which is greater than the temporal (T) [12]. Figure 1 (b) represents a clinical evaluation of the ISNT (inferior, superior, nasal, temporal) rule for a normal optic nerve, and Fig. 1 (c) shows a clinical evaluation of a glaucomatous optic nerve (right figure).

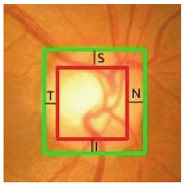
Analysis of blood vessel characteristics at the optic nerve head is also a useful quantitative tool for diagnosing and clinically managing glaucoma. The blood vessel ratio (BVR) is a measure that assesses the density of the blood vessels in the retina. In individuals with glaucoma, the progressive loss of nerve fibers leads to reduced blood vessel density, which results in a lower BVR [5]. Figure 1 (d) represents a glaucomatous optic nerve with less dense blood vessels.



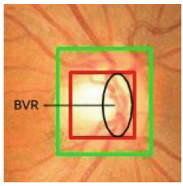
(a) Detail of the optic nerve [10]



(b) ISNT rule I >S >N >T - Normal eye [10]



(c) ISNT rule I >S >N >T - Glaucomatous eye [10]



(d) Blood Vessel Density (BVR) - Glaucomatous eye [10]

Fig. 1. Examples of optic nerves

3 Related Work

This section presents the set of works most related to our proposal. There are different works aimed at solving the glaucoma detection problem [2,11,18], which can be divided into two approaches: (1) deep learning neural networks; and (2) image processing. We discuss the main proposals of each of them below.

Several papers focus on using deep learning-based approaches [11]. In [25], an ensemble network was proposed for optical disk and optical cup segmentation. The ensemble network consists of eight networks, such as Mask-RCNN, M-Net, etc. Different data augmentation methods were used for each network, such as blurring and multi-scale detail manipulation. Each network learns different aspects of the data, and then a voting algorithm is designed to combine the results of these models. In [22], an investigation is performed into the applicability of pre-trained convolutional neural networks (CNNs) for glaucoma diagnosis by extracting features from high-level abstractions of retinal fundus images. The proposed system has been validated on high-resolution fundus (HRF), a publicly available database. The results show that among other pre-trained CNNs, the VGG16 network is best suited for glaucoma diagnosis. In [15], the optic disc and optic cup are segmented using a modified U-Net architecture employing the pre-trained SEResNet50 for a glaucoma diagnosis based on the CDR. These methods, however, need a large amount of training data that may not be readily available and would require large amounts of graphics processing unit (GPU) memory to train while taking more prediction time [11].

Another classification methodology is by the use of image processing [11]. In [16], a technique based on the neuroretinal kidney (NRR) Otsu segmentation is proposed where the disease is confirmed by calculating the CDR, rim-to-disc ratio (RDR), ISNT ratio, using SVM as a classifier in identifying glaucoma. In [9], the damage caused during glaucoma to the retinal nerve fiber layer is detected using computer-aided detection (CAD) and Gabor filtering. In [17], a series of features such as CDR ratio, the ratio of optic nerve head displacement distance to optic disc diameter, and the ratio of blood vessel area on the ISNT were used to classify the available retinal fundus images as normal and glaucoma images using a neural network classifier. In [8], based on line profile analysis, the cup-to-disc ratio is measured in retinal images. In [18], an automatic segmentation technique based on mathematical morphology has been used to diagnose glaucoma. In [7], a technique involves extracting and removing blood vessels using a hat transform and an internal painting process. A circular Hough transform is applied to the detected edges to obtain a coarse boundary of the optic disc. Then, the probable points of the optic disc are fed to a curve-fitting algorithm that uses a higher-order polynomial to draw the final boundary of the optic disc. Although these methods show good diagnostic accuracy, with the added advantage of not requiring much training data compared to deep learning models [11], they still have a high computational cost associated with feature extraction.

4 Proposed Solution

Our goal is to provide mechanisms that allow the extraction of features that can serve as medical support in diagnosing glaucoma. As previously mentioned, the attributes of fundus images must be extracted using minimal computational resources, which is our proposal's focus. In a simplified way, our proposal can be defined in the following steps:

1. Find the region of interest (optic nerve region) and perform its isolation/cutting;
2. Apply the CLAHE algorithm from the scikit-image library, resulting in the standardization and improvement of contrast and, consequently, the enhancement of image details;
3. Perform segmentation of the optical disk (delimitation of its edges) by detecting the most prominent contour of the normalized/equalized image using the OpenCV library;
4. Perform the segmentation of the optic disc's canopy (delimiting its edges) using the same principle as for the segmentation of the optic disc but with a different threshold value;
5. With the segmentations performed (edges defined), the attributes referring to the vertical and horizontal ratios of the disk cup, generating the CDRV and CDRH attributes, respectively, are calculated;
6. By analyzing the image of the optic nerve, we also extract the information on whether the eye in question is right or left by storing it in an attribute that we define as Eye;

7. The integrity of the optic nerve ISNT pattern is checked by comparing the Inferior, Superior, Nasal, and Temporal quadrants. The values are stored in the attributes IgtS (Inferior greater than Superior), IgtN (Inferior greater than Nasal), IgtT (Inferior greater than Temporal), SgtN (Superior greater than Nasal), SgtT (Superior greater than Temporal) and NgtT (Nasal greater than Temporal), with values of true or false; and
8. The density of the blood vessels related to the BVR is extracted by dividing the optic disc into quadrants (left and right). A count of pixels in the red hue is performed and compared to the area of the optical disk. The calculated value is stored in an attribute named BVR.

First, all attributes are extracted from a database containing previously classified images and adequately tabulated. This data is used to train a classical classifier, the SVM [13], which will generate a classification model. Then, for each eye image not yet analyzed, the same steps described above are performed to define the attributes of this new eye, which in turn must be classified by the generated model.

In the following subsections, the main steps mentioned above will be detailed.

4.1 Optic Nerve Isolation

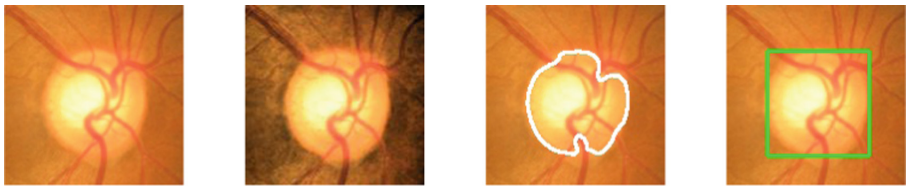
Isolation of the optic nerve is performed using the following process:

1. The original image is reduced to one-fifth of its height, keeping the dimensions proportional to the width;
2. The reduced image is subjected to a CLAHE technique for enhancement of local image contrast and detail enhancement; and
3. The nerve is isolated by an algorithm that, starting from the center of this reduced image (cx, cy), searches for the brightest point in an area delimited by a rectangle of vertices $[(cx - N, cy - N), (cx + N, cy + N)]$, where N is 1/12 of the height of the reduced image. It is then checked whether the sum of the color channels (R, G, and B) of the brightest point obtained in the bounded area is greater than 700. If so, the coordinates (cx, cy) are defined to the selected point, and the isolated optic nerve is defined in a rectangle with vertices $[(cx - 75, cy - 75), (cx + 75, cy + 75)]$ of the original image, resulting in an image of 150×150 pixels. Otherwise, the value of N is increased by 1/12 of the reduced image's height and repeated until an isolated optic nerve is reached. Figure 2 (a) represents the isolated optic nerve using the algorithm.

4.2 Optical Disc Segmentation

From the image of the isolated optic nerve, the process of segmenting the optic disc (delimiting the ends) is started:

1. The CLAHE is applied, as shown in Fig. 2 (b);



(a) Isolated nerve (b) Equalized isolated nerve (c) Increased disc contour (d) Segmented disc (delimited ends)

Fig. 2. Isolation of the Optic Nerve and Segmentation (Delimitation of the Extremities) of the Optic Disc [10]

2. Next, the proposed algorithm performs the binarization of the equalized image and, through the findContours method from the OpenCV library, searches for and returns the largest contour in the image;
3. This contour is then drawn on the image of the isolated nerve, and its points are used to delimit the ends of the optic disc (Fig. 2 (c)); and
4. A rectangle is drawn at the endpoints of the contour and the optic disc is defined as in Fig. 2 (d).

4.3 Disc Cup Segmentation

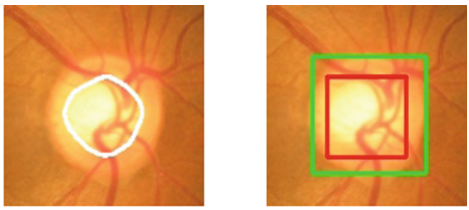
The disk canopy is segmented (defining its edges) following the same principle as the disk segmentation, with the following change:

1. The algorithm performs binarization of the equalized image using another threshold value, seeking greater emphasis on the internal region, with higher brightness, and through the method findContours, from the OpenCV library, search and return the largest contour of the image;
2. This contour is then drawn on the image of the isolated nerve, and its points are used to delimit the extremities of the disk cup, as in Fig. 3 (a); and
3. A rectangle is drawn at the endpoints of the contour and the canopy of the optical disc is defined as in Fig. 3 (b).

4.4 Setting the Eye Direction

To define whether the eye is Right or Left, the following steps are followed:

1. The enhanced/equalized optic nerve image is split vertically;
2. Each of the parts (right and left) is scanned pixel by pixel, counting the brightest pixels in the red and green channels;
3. The total number of pixels found is compared, and the direction of the eye is set on the part containing the greatest number of counted pixels; and
4. The Eye attribute is then set to 0 for the left eye and 1 for the right eye.



(a) Biggest cup contour (b) Segmented cup (Delimited Ends)

Fig. 3. Segmentation (edge delimitation) of the optical disc Cup [10]

5 Proposal Evaluation

5.1 Environment

To evaluate our proposal, we considered the ORIGA image bank [26], provided by [10], composed of 650 fundus images of the eye, being 482 healthy and 168 glaucomatous. All steps of our experimentation (feature extraction and instance classification) were performed in the following environment: computer with Intel(R) Core (TM) i5-6500 CPU @ 3.20 GHz, 8 GB RAM, 480 GB SSD, and Linux Ubuntu 20.04 operating system. Ten-fold cross-validation was used as a technique for separating training and test data. SVM was used to classify the images using the following parameters: cost = 9, kernel = poly, degree = 8, gamma = scale, coefficient = 0.5. 650 images were processed in 437.27 s, representing an average processing time of approximately 0.67 s for each image.

5.2 Results

From the effectiveness point of view, we considered the metrics Accuracy, Recall, Precision, and F1-Score, commonly used to evaluate classification algorithms. After the cross-validation process (ten folds) considering only the tabulated attributes, Vertical CDR and Eye Direction, provided along with the dataset, and considering all the attributes extracted in the new proposal (Eye, Vertical CDR, Horizontal CDR, IgtS, IgtN, IgtT, SgtN, SgtT, NgtT, BVR), we found the values according to Table 1.

Table 1. Results obtained from tabulated attributes supplied with the dataset vs. results of the new proposal

Attributes	Accuracy	Recall	Precision	F1-Score
Supplied with the dataset	0.7430	0.0297	0.5555	0.6458
New Proposal	0.9153	0.7321	0.9248	0.8172

From the point of view of model interpretability, two (2) explainability techniques were analyzed, SHAP [14] (global analysis), and LIME [19] (local analysis).

Based on game theory, SHAP assigns each attribute an importance value for a specific prediction in the [14] model. The idea of this method is that the attributes of an instance are "players," and the "final score" is related to the performance of all the "players" in predicting the model. This method showed the attributes SgtT, IgtT, and BVR as the main contributors (with the highest weight) to the model predictions, as per Figs. 4 and 5.

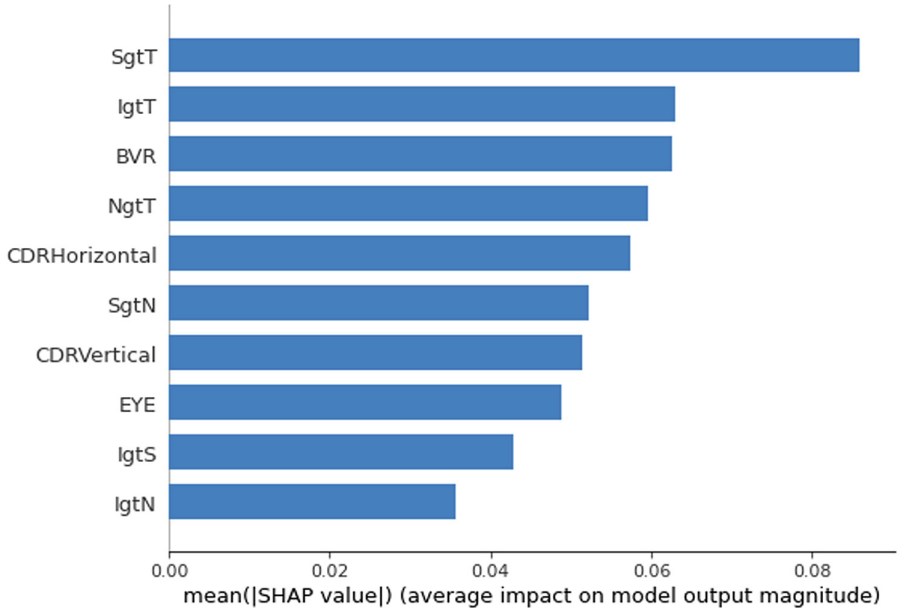


Fig. 4. SHAP values chart for attributes in descending order of importance

LIME, on the other hand, interprets individual instance predictions based on the local approximation of the model around a given prediction [19]. This method showed, for the second instance of the model, for example, the attributes NgtT, SgtT, and SgtN as the main contributors (of most significant weight) to the prediction, as per Figs. 6 and 7.

Analyzing the explanations generated by the SHAP and LIME methods, we found that the attributes with the most significant contribution to the model prediction were attributes extracted by the proposal of this paper.

We manually inspected some misclassified images and found that the feature extraction needed to be performed correctly. We show some examples in Fig. 8.

As the dataset used (ORIGA) has an image database with the official markings defined (quantitative characteristics duly annotated), a comparison process

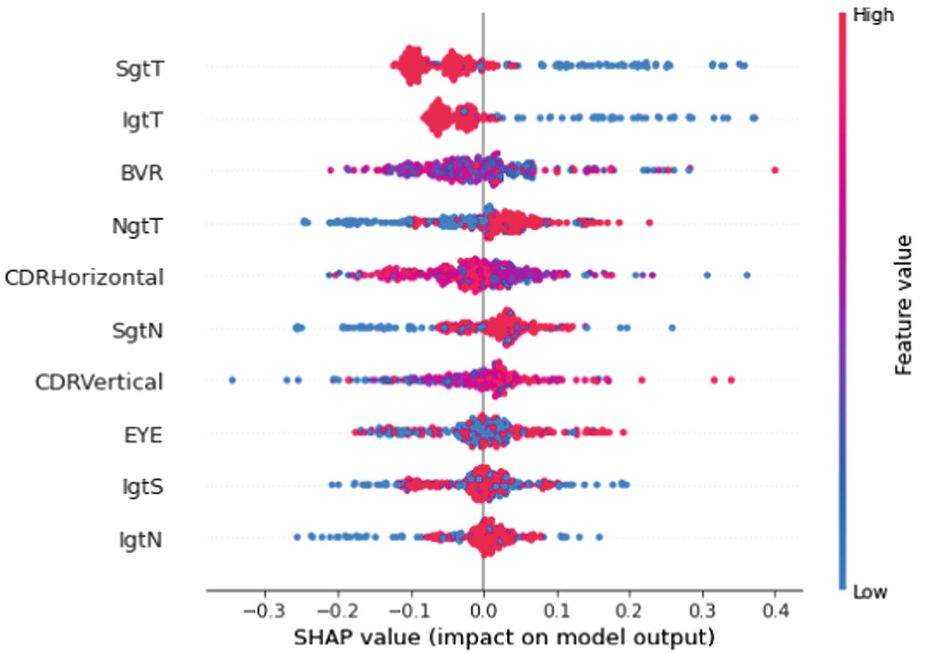


Fig. 5. SHAP values chart with the contribution of each attribute for all database instances

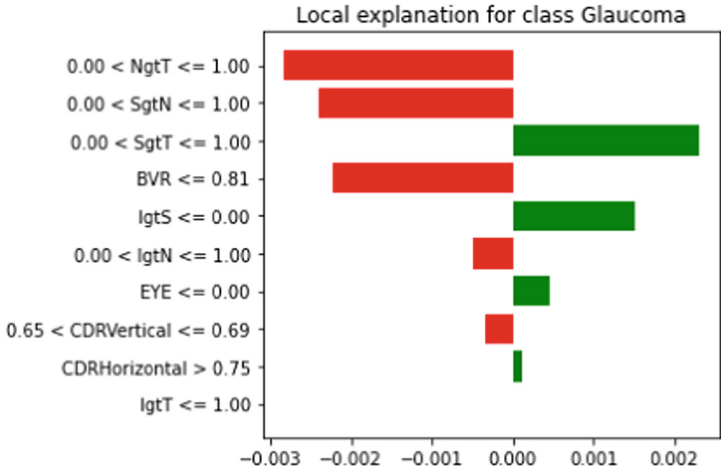


Fig. 6. LIME plot of the contribution of each attribute to the prediction of the second instance of the model

by cosine similarity was done between the official segmentation data (optical disk location and disk cup) and the data obtained by the segmentation method proposed in this paper, being possible to make the classification of the images

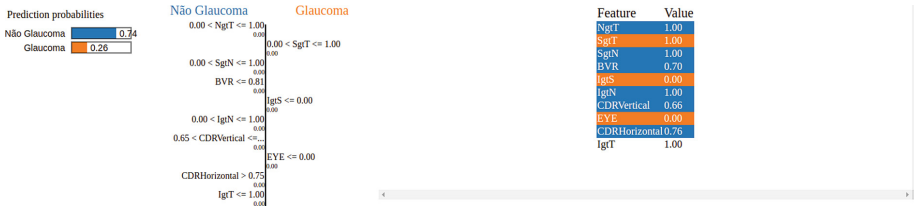


Fig. 7. LIME plot for the explanation of one instance of the model (second instance)



Fig. 8. Failure in the segmentation process Source: Figs. 224, 335 and 594 [10]

using the images that were better segmented. In this way, new classifications were made with varying similarity indices. The results can be seen in Table 2. In our results, we observed that the performance metrics presented significant improvement. The more accurate the extraction of features, the greater the accuracy of the classifier, pointing to future directions of work to be presented in the next section.

Table 2. Table with results with similarity level

Similarity	Total Images	Accuracy	Recall	Precision	F1-Score
80%	641	0.9157	0.7500	0.9044	0.8200
85%	504	0.9246	0.7615	0.9339	0.8389
90%	445	0.9325	0.8034	0.9306	0.8623
95%	257	0.9766	0.9218	0.9833	0.9516

6 Conclusion and Future Works

Glaucoma is a disease that progressively affects the optic nerve, the leading cause of irreversible blindness worldwide. One of the most assertive strategies to make the diagnosis is the OCT, which identifies anomalies in the optic nerve anatomy. OCT is a high-cost test, so some work in the literature has been using

computationally expensive deep neural networks to analyze fundoscopy (retinal fundus) images for glaucoma diagnosis. As an alternative to these approaches, in this work, we proposed and implemented a low-cost computational method to extract features of the optic nerve anatomy (i.e., optic cup and disc segmentation) by processing retinal fundus images, which is used in conjunction with low computational cost classification algorithms (i.e., SVM), being able to perform an accurate diagnosis. More specifically, the more accurate the feature extraction, the higher the accuracy of the classifier.

As future work, we point out the need to improve the image normalization process and the segmentation steps of the optical disc and the disc cup for an improvement in the segmentation process. We also point out the need to perform new experiments with other publicly available datasets and thus be able to perform a broader evaluation of the solution proposed in this article.

References

1. Bradski, G.: The OpenCV library. Dr. Dobb's J. Softw. Tools (2000)
2. Camara, J., Neto, A., Pires, I.M., Villasana, M.V., Zdravevski, E., Cunha, A.: Literature review on artificial intelligence methods for glaucoma screening, segmentation, and classification. J. Imaging **8**(2), 19 (2022). https://doi.org/10.3390/jimaging8020019, https://www.mdpi.com/2313-433X/8/2/19
3. D'Angelo, G., Palmieri, F., Robustelli, A., Castiglione, A.: Effective classification of android malware families through dynamic features and neural networks. Connect. Sci. **33**(3), 786–801 (2021). https://doi.org/10.1080/09540091.2021.1889977
4. D'Angelo, G., Rampone, S.: Diagnosis of aerospace structure defects by a HPC implemented soft computing algorithm. In: 2014 IEEE Metrology for Aerospace (MetroAeroSpace), pp. 408–412 (2014). https://doi.org/10.1109/MetroAeroSpace.2014.6865959
5. Deepika, E., Maheswari, S.: Earlier glaucoma detection using blood vessel segmentation and classification. In: 2018 2nd International Conference on Inventive Systems and Control (ICISC), pp. 484–490 (2018). https://doi.org/10.1109/ICISC.2018.8399120
6. D'Angelo, G., Castiglione, A., Palmieri, F.: A cluster-based multidimensional approach for detecting attacks on connected vehicles. IEEE Internet Things J. **8**(16), 12518–12527 (2021). https://doi.org/10.1109/JIOT.2020.3032935
7. Gopalakrishnan, A., Almazroa, A., Raahemifar, K., Lakshminarayanan, V.: Optic disc segmentation using circular Hough transform and curve fitting. In: 2015 2nd International Conference on Opto-Electronics and Applied Optics (IEM OPTRONIX), pp. 1–4. IEEE (2015). https://doi.org/10.1109/OPTRONIX.2015.7345530
8. Hatanaka, Y., et al.: Automatic measurement of cup to disc ratio based on line profile analysis in retinal images. In: 2011 Annual International Conference of the IEEE Engineering in Medicine and Biology Society, pp. 3387–3390. IEEE (2011). https://doi.org/10.1109/IEMBS.2011.6090917
9. Hayashi, Y., et al.: Detection of retinal nerve fiber layer defects in retinal fundus images using Gabor filtering. In: Giger, M.L., Karssemeijer, N. (eds.) Medical Imaging 2007: Computer-Aided Diagnosis, vol. 6514, p. 65142Z. International Society for Optics and Photonics, SPIE (2007). https://doi.org/10.1117/12.710181

10. Kaggle Inc.: Glaucoma detection (2022). https://www.kaggle.com/datasets/sshikamaru/glaucoma-detection
11. Krishnan, R., Sekhar, V., Sidharth, J., Gautham, S., Gopakumar, G.: Glaucoma detection from retinal fundus images. In: 2020 International Conference on Communication and Signal Processing (ICCSP), pp. 0628–0631. IEEE (2020). https://doi.org/10.1109/ICCSP48568.2020.9182388
12. Kumar, B.N., Chauhan, R.P., Dahiya, N.: Detection of glaucoma using image processing techniques: a review. In: 2016 International Conference on Microelectronics, Computing and Communications (MicroCom), pp. 1–6. IEEE (2016). https://doi.org/10.1109/MicroCom.2016.7522515
13. Lin, K.C., Liu, T.Y., Chen, P.H., Lin, C.T.: Use support vector machine (SVM) to estimate gas concentration in mixture condition. In: 2017 International Conference on Applied System Innovation (ICASI), pp. 744–746. IEEE (2017). https://doi.org/10.1109/ICASI.2017.7988537
14. Lundberg, S.M., Lee, S.I.: A unified approach to interpreting model predictions. In: Guyon, I., et al. (eds.) Advances in Neural Information Processing Systems, vol. 30, pp. 4765–4774. Curran Associates, Inc. (2017). http://papers.nips.cc/paper/7062-a-unified-approach-to-interpreting-model-predictions.pdf
15. Maadi, F., Faraji, N., Bibalan, M.H.: A robust glaucoma screening method for fundus images using deep learning technique. In: 2020 27th National and 5th International Iranian Conference on Biomedical Engineering (ICBME), pp. 289–293. IEEE (2020). https://doi.org/10.1109/ICBME51989.2020.9319434
16. Naga Kiran, D., Kanchana, V.: Recognistion of Glaucoma using OTSU segmentation method (2019)
17. Nayak, J., Acharya, U.R., Bhat, P., Shetty, N., Lim, T.C.: Automated diagnosis of Glaucoma using digital fundus images. J. Med. Syst. **33**, 337–46 (2009). https://doi.org/10.1007/s10916-008-9195-z
18. Pal, S., Chatterjee, S.: Mathematical morphology aided optic disk segmentation from retinal images. In: 2017 3rd International Conference on Condition Assessment Techniques in Electrical Systems (CATCON), pp. 380–385. IEEE (2017). https://doi.org/10.1109/CATCON.2017.8280249
19. Ribeiro, M.T., Singh, S., Guestrin, C.: "Why should I trust you?": explaining the predictions of any classifier. In: Proceedings of the 22nd ACM SIGKDD International Conference on Knowledge Discovery and Data Mining, San Francisco, CA, USA, 13–17 August 2016, pp. 1135–1144 (2016)
20. Sarhan, M.H., et al.: Machine learning techniques for ophthalmic data processing: a review. IEEE J. Biomed. Health Inform. **24**(12), 3338–3350 (2020). https://doi.org/10.1109/JBHI.2020.3012134
21. Stefan, A.M., Paraschiv, E.A., Ovreiu, S., Ovreiu, E.: A review of glaucoma detection from digital fundus images using machine learning techniques (2020). https://doi.org/10.1109/EHB50910.2020.9280218
22. Sushil, M., Gnanaprakasam, S., Rajan, L., Devi, N.: Performance comparison of pre-trained deep neural networks for automated glaucoma detection, January 2019. https://doi.org/10.1007/978-3-030-00665-5-62
23. Vessani, R.M.: Comparação entre diversas técnicas de imagem para diagnóstico do glaucoma, Faculdade de Medicina, Universidade de São Paulo (2008). https://doi.org/10.11606/T.5.2008.tde-02062008-112610
24. Van der Walt, S., et al.: Scikit-image: image processing in Python. PeerJ **2**, e453 (2014)
25. Yin, P., et al.: Optic disc and cup segmentation using ensemble deep neural networks (2018)

26. Zhang, Z., et al.: ORIGA(-light): an online retinal fundus image database for glaucoma analysis and research. In: Conference Proceedings : ... Annual International Conference of the IEEE Engineering in Medicine and Biology Society. IEEE Engineering in Medicine and Biology Society. Conference 2010, p. 3065-8, August 2010. https://doi.org/10.1109/IEMBS.2010.5626137
27. Zhao, R., Chen, X., Liu, X., Chen, Z., Guo, F., Li, S.: Direct cup-to-disc ratio estimation for glaucoma screening via semi-supervised learning. IEEE J. Biomed. Health Inform. **24**(4), 1104–1113 (2020). https://doi.org/10.1109/JBHI.2019.2934477